Solomon, I. (1955) *Phys. Rev. 99*, 559–565.
Sundaralingam, M. (1969) *Biopolymers 7*, 821–860.
Syed, D. B., Strauss, R. S., Ashton, R. W., & Sloan, D. L. (1985) *Fed. Proc., Fed. Am. Soc. Exp. Biol. 44*, 672.
Tinkham, M., Weinstein, R., & Kip, A. F. (1951) *Phys. Rev. 84*, 848–849.
Umezu, K., Amaya, T., Yashimoto, A., & Tomita, K. (1971) *J. Biochem. (Tokyo) 70*, 249–269.
Victor, J., Greenberg, L. B., & Sloan, D. L. (1979a) *J. Biol. Chem. 254*, 2647–2655.
Victor, J., Leo-Mensah, A., & Sloan, D. L. (1979b) *Biochemistry 18*, 3597–3604.

NMR Studies of the Interaction of Chromomycin A_3 with Small DNA Duplexes I†

Max A. Keniry,‡ Stephen C. Brown,‡,§ Elisha Berman,‖ and Richard H. Shafer*,‡
Department of Pharmaceutical Chemistry, School of Pharmacy, University of California, San Francisco, California 94143, and Department of Organic Chemistry, The Weizmann Institute of Science, 76100 Rehovot, Israel
Received July 3, 1986; Revised Manuscript Received October 30, 1986

ABSTRACT: ^1H and ^{31}P NMR spectral analysis of a chromomycin/d(ATGCAT)$_2$ complex provides strong evidence for a nonintercalative mode of drug binding. Investigation of the imino proton region of the duplex suggests a protection of one of the two guanine imino protons from fast exchange with the bulk water up to at least 45 °C by the drug. Subsequent one-dimensional nuclear Overhauser enhancement experiments place the exchangeable chromomycin chromophoric hydroxyl proton <0.45 nm from this guanine imino proton and the chromophore 7-methyl <0.45 from the internal thymine 6-proton and/or the guanine 8-proton. ^1H two-dimensional NMR reveals that the duplex retains a right-handed B conformation but there are distortions at the TGC region of one chain and large deviations in the chemical shift of protons relative to the uncomplexed duplex in the other chain in the same TGC region. The data suggest that the chromomycin chromophore is oriented such that the hydrophilic side of the ring system is proximal to the helix center in the major groove near the TG region while the aromatic side of the ring is oriented away from the helix but is partially protected from the solvent by the aliphatic chain, which bends back over the two aromatic protons. Changes in the ^{31}P spectrum of the duplex on binding of the drug are different from the effect of either actinomycin or netropsin on nucleic acid fragments.

Chromomycin and the related antibiotics mithramycin and olivomycin are potent inhibitors of in vitro and in vivo DNA[1]-directed RNA synthesis via complex formation with DNA, in the presence of Mg^{2+} (Miyamoto et al., 1966; Berlin et al., 1966; Bakhaera et al., 1968; Wakisaka et al., 1963; Kersten et al., 1967; Kersten & Kersten, 1974; Slavek & Carter, 1975; Remers, 1979; Gause, 1965). They exhibit antitumor behavior against a variety of experimental tumors, although their potential utility is limited by their toxicity (Gause, 1965) and immunosuppressive properties (Imai et al., 1970; Lvashenko & Kolesnikova, 1965). A detailed three-dimensional picture of the structure of the complex appears essential for elucidating the detailed biological action of this antibiotic. Since both chromomycin and a chromomycin/nucleotide complex have eluded X-ray crystal analysis to this present time, one-dimensional and two-dimensional nuclear magnetic resonance (NMR) techniques become the method of choice for determining these structures.

In the past 2 decades, a variety of techniques has been applied to the binding properties of chromomycin to DNA. There is an absolute requirement for 2-aminopurine residues such as guanine (Ward et al., 1965; Cerami et al., 1967) prompting comparisons with actinomycin. A direct and tight noncovalent binding to guanine-containing DNA is not disputed (Behr & Hartmann, 1965; Kersten, 1965; Cobreros et al., 1982). Helicity in the DNA is a requirement for binding; separated strands show no interaction with chromomycin (Behr et al., 1969). However, the position and mode of the binding remain a matter of controversy. No doubt, the apparent similarity of binding properties with actinomycin (which has been shown to intercalate; Brown et al., 1984) has prompted some to propose an intercalative mode of binding for chromomycin (Behr et al., 1969; Horwitz & McGuire, 1978), but there is evidence to suggest a different mode of binding. Chromomycin does not alter the sedimentation coefficient of normal double-stranded DNA (Cobreros et al., 1982), and unlike actinomycin, it does not induce unwinding and rewinding of the double helix in supercoiled DNA (Waring, 1970). Recent ^{13}C and ^1H NMR studies of drug complexes with fragments of calf thymus DNA, however, produced additional evidence of similarity between the binding of actinomycin and chromomycin and new support for the interca-

† Supported in part by U.S. Public Health Service Grant CA 27343 awarded by the National Cancer Institute, DHHS, and Grant 84-00011 from the U.S.–Israel Binational Science Foundation. This work has benefitted through the use of facilities made available to the School of Pharmacy (NIH Grants RR01668 and RR01695 and NSF Grant DMB8406826).
‡ University of California.
§ Present address: Department of Biology, University of Pennsylvania, Philadelphia, PA 19104.
‖ The Weizmann Institute of Science.

[1] Abbreviations: ACTD, actinomycin D; CRA, chromomycin A_3; COSY, ^1H two-dimensional *J*-correlation NMR; DNA, deoxyribonucleic acid; EGTA, ethylene glycol bis(β-aminoethyl ether)-*N,N,N',N'*-tetraacetic acid; FID, free induction decay; HOHAHA, homonuclear Hartmann–Hahn relayed spectroscopy; HPLC, high-pressure liquid chromatography; NMR, nuclear magnetic resonance; NOE, nuclear Overhauser enhancement; NOESY, ^1H two-dimensional NOE correlation NMR in the pure absorption mode; RNA, ribonucleic acid; 2D, two dimensional.

0006-2960/87/0426-1058$01.50/0

lation of chromomycin (Berman & Shafer, 1983; Berman et al., 1985).

The introduction of a multitude of two-dimensional NMR techniques (Aue et al., 1976; Freeman & Morris, 1979; Muller et al., 1975; Maudsley & Ernst, 1977; Bax et al., 1981; Wuthrich et al., 1982; Davis & Bax, 1985), the use of small mainframe computers to process the large data sets, and the employment of computer graphics supplemented with statistical mechanical calculations have made the NMR technique a viable alternative to X-ray crystal structure analysis for the elucidation of the 3D structure of small proteins and drug/nucleotide complexes. The preliminary solution structures of some proteins (Braun et al., 1981) and two drug/nucleic acid complexes have been determined (Brown et al., 1984; Patel & Shapiro, 1986). This paper is the first in a systematic attempt at determining the binding site of chromomycin to guanine-containing nucleic acid fragments and the structural changes induced in chromomycin and the nucleic acid fragment. No crystal structure of either chromomycin or a chromomycin/nucleic acid complex exists, and furthermore, the mode of binding is undetermined, making this a logical extension of our actinomycin/d(ATGCAT)$_2$ work (Brown et al., 1984). We present evidence to suggest a nonintercalative mode of binding in the major groove with the hydrophilic side of the chromophoric ring proximal to the helix center and the hydrophobic side oriented away from the helix.

Experimental Procedures

Chromomycin A_3 was purchased from Boehringer Mannheim (Mannheim, West Germany) and Sigma (St. Louis, MO) and used without further purification. d(ATGCAT) was synthesized by standard triester methods (Narang et al., 1980). The purity was checked by ^{1}H NMR, ^{31}P NMR, HPLC, and base composition analysis. The complex was made up to final concentrations of chromomycin (4 mM), d(ATGCAT) (8 mM), and Mg^{2+} (20 mM) in either phosphate buffer (100 mM phosphate, 180 mM NaCl, 0.2 mM EGTA, pH 8.2) or borate buffer (100 mM borate, 180 mM NaCl, 0.2 mM EGTA, pH 8.2).

NMR Experimental Parameters. All ^{1}H spectra were collected on the GN-500 NMR spectrometer (General Electric, Fremont, CA) at the Univeristy of California, San Francisco, CA, at a proton frequency of 500.0 MHz. A 90° pulse width of 13 μs and a recycle delay of 5 s or longer were used unless otherwise stated.

(A) One-dimensional spectra of the low-field region (10–16 ppm) containing the imino protons of d(ATGCAT)$_2$ and the hydroxyl proton of chromomycin were obtained with a $1\bar{3}3\bar{1}$ pulse sequence (Hore, 1983). NOE data in the same region were obtained in the interleaved mode by taking the difference spectra from data sets with an on-resonance and off-resonance selective preirradiation pulse of 250 ms. All NOE data of exchangeable protons were collected at 2 °C.

(B) Two-dimensional NOESY spectra were acquired in the pure absorption mode (States et al., 1982) with 4K data points in the t_2 dimension stored in alternate blocks and 512 FID's in the t_1 dimension. FID's were apodized with a 45° sine bell in both dimensions and also zero filled once in each dimension. The base lines of the spectra were corrected to a sixth-order polynominal in ω_1 and ω_2 (Pearson, 1977; Basus, 1984). All processing of 2D data sets was performed on a VAX 11/750 (Digital Equipment Corp., Maynard, MA) at the Univeristy of California, San Francisco, CA.

Homonuclear scalar connectivity was determined by a COSY experiment (Aue et al., 1976) and by two-dimensional homonuclear Hartmann–Hahn relayed spectroscopy (HOHAHA; Davis & Bax, 1985). The latter experiment was performed in the pure absorption mode (States et al., 1982) with 4K data points in the t_2 dimension stored in alternate blocks and 512 FID's in the t_1 dimension. FID's were apodized by exponential multiplication with a weighting factor of 7 Hz in the t_2 dimension and 14 Hz in the t_1 dimension and one zero fill in each dimension.

(C) ^{31}P spectra were collected at 97.5 MHz on a home-built wide-bore 5.6-T instrument equipped with a Nicolet 1180 data system and a 293B pulse programmer (Univeristy of California, San Francisco). All spectra were collected with broad-band proton decoupling over a 2500-Hz sweep width with a 60° pulse (90° pulse widths were 45 μs) and a 2.8-s recycle time. Chemical shifts were referenced to an external capillary of 0.85% phosphoric acid.

Results and Discussion

We have chosen d(ATGCAT) as the first model nucleotide fragment for a structural study of a nucleic acid/chromomycin complex for several reasons: first, the ACTD/d(ATGCAT) has been thoroughly characterized, particularly by NMR techniques (Patel, 1974, 1978; Brown et al., 1984); second, it has been suggested ACTD and CRA have similar modes of binding (Behr et al., 1969; Horwitz & McGuire, 1978); third, it contains two symmetric GC pairs, at least one GC pair being necessary for binding (Ward et al., 1965; Cerami et al., 1967); fourth, it closely resembles one of the binding sequences, 5′AT-GCT-T, determined by footprinting techniques (Van Dyke & Dervan, 1983), and finally, it changes the intensity of the absorption peak and experiences slow kinetics on binding just as in the binding of natural DNA to chromomycin/Mg^{2+} (data not shown).

Imino Proton Region. The temperature dependence of imino proton exchange in duplex d(ATGCAT) proceeds as expected. The external A-T imino protons exchange broaden by 15 °C (Figure 1A), and by 25 °C, the internal A-T imino protons are unobservable (Figure 1A) while the G-C imino protons broaden substantially (Figure 1A). The addition of chromomycin removes the degeneracy of the G-C imino protons (Figure 1B), but the internal A-T imino protons (Figure 1B) and the external A-T imino protons (observable at 2 °C, Figure 2A) are either not split by the presence of chromomycin or too broad to show any splitting. The chromomycin chromophoric hydroxyl proton is also clearly observable at 16.12 ppm. By 20 °C, the internal A-T imino protons and one G-C imino proton are partially exchange broadened (Figure 1B). By 25 °C, only the chromomycin hydroxyl and the other G-C imino proton are observable (Figure 1B). Neither of these protons has exchange broadened by 45 °C (spectrum not shown, Table I), suggesting a protection of this site from fast exchange with bulk water by the drug. It is likely that the duplex is held intact, at least at this protected site, by the drug up to at least 45 °C since Behr et al. found base pairing a necessary requirement for chromomycin binding to poly(dG)·poly(dC) (Behr et al., 1969). We do not, however, rule out a disruption of the helix at this point and formation of a direct hydrogen bond of the G-C imino proton with the chromomycin chromophore.

The spatial proximity of exchangeable protons to each other was determined by 1D NOE experiments. Since the nuclear Overhauser effect has an inverse sixth power dependence on interproton distance, it may be used to identify proton pairs with interproton distances in the range 0.2–0.45 nm (Noggle & Schirmer, 1971). Irradiating the internal A-T imino protons for 250 ms results in approximately equal intensity peaks for the G-C imino protons (Figure 2C). This confirms that

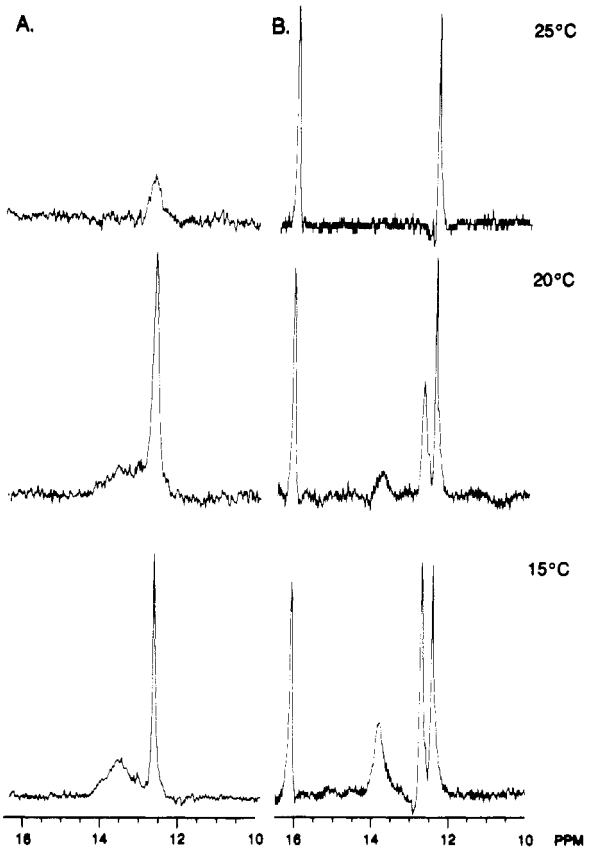

FIGURE 1: Temperature dependence of the low-field region of (A) d(ATGCAT)$_2$, 4 mM, in pH 8.0 100 mM borate, 180 mM NaCl, and 0.2 mM EGTA at 15, 20, and 25 °C and (B) chromomycin/d-(ATGCAT)$_2$ (1:1) (4 mM) in pH 8.2 100 mM borate, 180 mM NaCl, 0.2 mM EGTA, and 20 mM Mg^{2+} at 15, 20, and 25 °C. Spectra were collected in 300–600 scans over a spectral width of 14 000 Hz. A digital line broadening of 5 Hz was used.

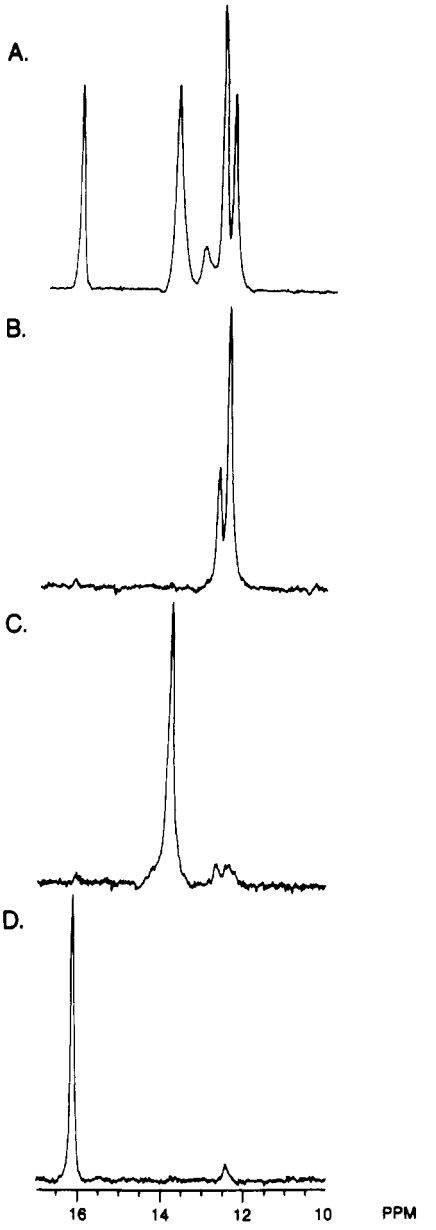

FIGURE 2: (A) CRA/d(ATGCAT)$_2$, 4 mM, in pH 8.2 100 mM borate, 180 mM NaCl, 0.2 mM EGTA, and 20 mM Mg^{2+} at 2 °C. NOE difference spectra after 250-ms irradiation at (B) 12.4 ppm (upfield G-C imino proton), (C) 13.8 ppm (internal A-T imino proton), and (D) 16.1 ppm (chromomycin chromophore 9-OH proton). Spectra typically required 400 scans at a recycle time of 5.8 s over a sweep width of 14 kHz.

near-normal base stacking remains between the A-T and the G-C pairs. It is not possible to check the integrity of the base stacking between the G-C pairs since the G-C imino proton resonance adjoining the irradiated resonance is sufficiently "tickled" by the preirradiation pulse to make the experimental results ambiguous. On irradiation of the chromomycin hydroxyl proton (16.12 ppm), an NOE is observed at the upfield G-C imino proton, which is also the proton that has been shifted by complexation with chromomycin (Figure 2D). Irradiating this same G-C proton results in a similar Overhauser enhancement to the chromomycin hydroxyl proton (Figure 2B). This places the hydrophilic side of the chromomycin chromophore within 0.45 nm of the center of one G-C pair. It is the first direct evidence suggesting that the guanine requirement of this drug may result from the interaction of the chromophore and a guanine imino proton.

Feigon et al. (1984) have shown that downfield shifts of imino protons are characteristic of minor groove binders. The upfield shift of the G-C imino proton on binding of chromomycin is evidence against this mode of binding. Although upfield complexation shifts are characteristic of intercalators, the imino proton resonances of the CRA/d(ATGCAT)$_2$ complex display anomalous behavior when compared to those in nucleotide complexes of proven intercalators, such as actinomycin (ACTD). The internal A-T imino proton resonance of the ACTD/d(ATGCAT)$_2$ complex moves upfield with temperature (Patel, 1974); in contrast, the same proton resonance in CRA/d(ATGCAT)$_2$ is invariant with temperature. Furthermore, both G-C imino protons in the ACTD/d-(ATGCAT)$_2$ complex move upfield with increasing temperature and broaden at approximately the same rate (Patel, 1974), but in the CRA/d(ATGCAT)$_2$ complex the unshifted G-C resonance moves downfield, broadens, and disappears by 25 °C, but the upfield shifted resonance moves further upfield only at high temperatures and broadens slowly (Table I). A classical intercalation model does not seem consistent with the "asymmetric effects" at just one of the G-C imino protons, although some penetration between the stacked nucleotides cannot be discounted by the imino proton data.

^1H Resonance Assignments by 2D NMR. One-dimensional spectra of d(ATGCAT)$_2$, chromomycin A$_3$, and chromomycin A$_3$/d(ATGCAT)$_2$ are shown in Figure 3, and the numbering scheme for the drug and the nucleotide and an expanded spectrum of the aromatic region are shown in Figure 4.

d(ATGCAT)$_2$ Resonances. The assignment strategy for identifying nucleotide resonances in spectra of the drug/nucleotide complex is similar to schemes that have been devised

Table I: Temperature Dependence of Imino Proton Region Chemical Shifts (in ppm) and Line Widths (in Parentheses) of CRA/d(ATGCAT)$_2$[a]

temp (°C)	AT_{ext}	AT_{int}	GC_a	GC_b	9-OH[b]
2	13.123 (70)	13.828 (41)	12.700 (21)	12.449 (24)	16.148
6	13.155	13.820 (69)	12.699 (17)	12.445 (17)	16.140
15		13.820 (99)	12.717 (24)	12.443 (16)	16.101
20			12.730 (49)	12.442 (16)	16.077
25				12.443 (19)	16.053
35				12.416 (20)	16.015
45				12.374 (25)	15.947

[a] All chemical shifts are reported relative to internal trimethylsilyl propionate. Line widths are the width at half-height in Hz. [b] This resonance has two components. Its line shape will be discussed in a later publication.

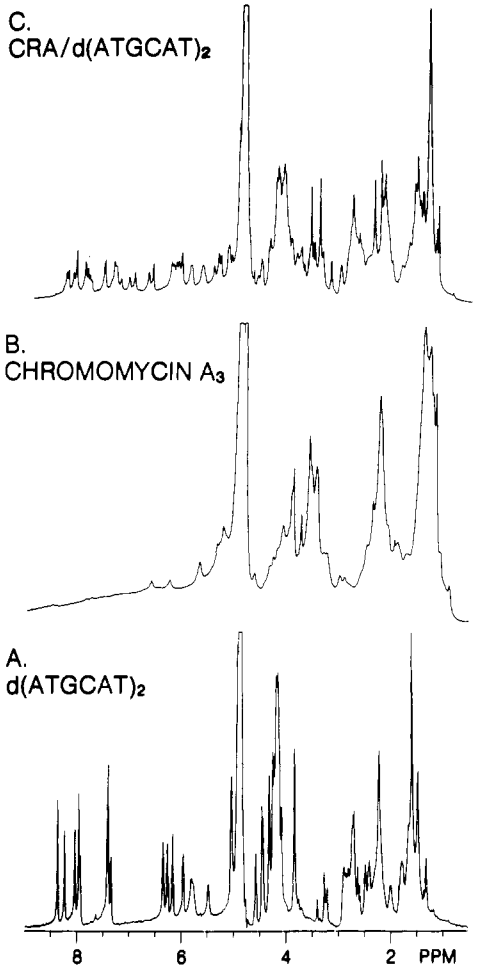

FIGURE 3: The 500-mHz ^{1}H spectra of (A) d(ATGCAT)$_2$, 4 mM, in pH 8.0 100 mM borate, 180 mM NaCl, and 0.2 mM EGTA at 15 °C, (B) chromomycin A_3, 3 mM, in pH 8.2, 100 mM phosphate, 180 mM NaCl, and 0.2 mM EGTA, and (C) chromomycin A_3/d-(ATGCAT)$_2$, 4 mM, in pH 8.2, 100 mM phosphate, 180 mM NaCl, and 0.2 mM EGTA.

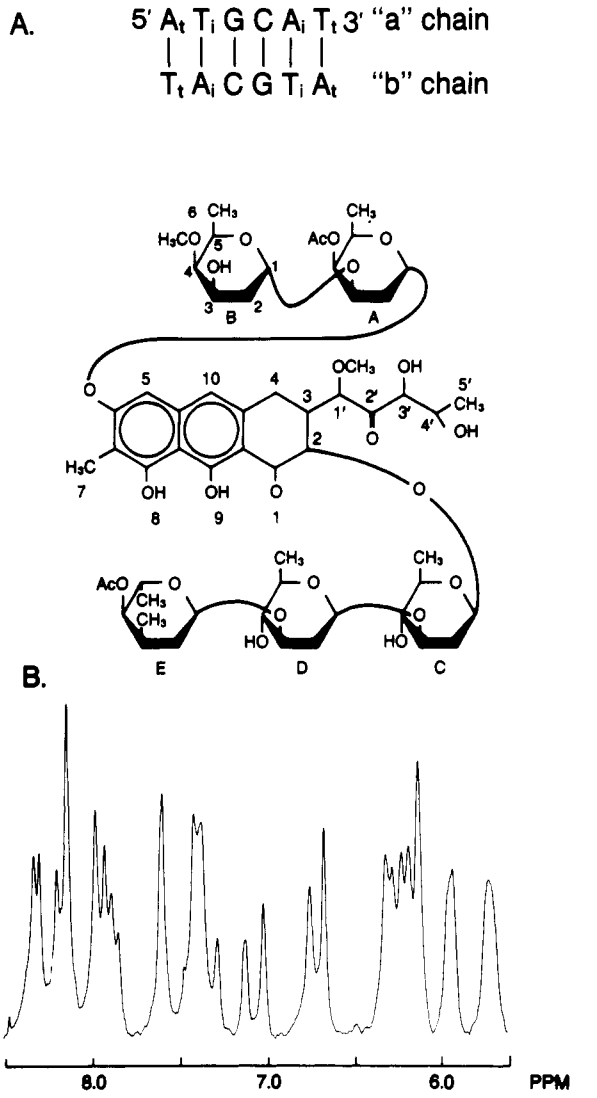

FIGURE 4: (A) Numbering system used for d(ATGCAT)$_2$ and chromomycin A_3 in the text, the latter being the same numbering scheme proposed by Thiem et al. (1979). The chromomycin sugar protons are identified by a letter denoting a particular sugar and a number specifying the proton on that sugar. All protons on the chromophore and the aliphatic chain are given the prefix Cr; e.g. the 7-methyl is denoted Cr7. Methoxy methyl groups are identified by the letter M; e.g., the B sugar methoxy is denoted BM. Acetyl methyl groups are identified by the subscript ac; e.g., A_{ac} is the symbol for the acetyl on the A sugar. (B) Aromatic region of the ^{1}H 500-mHz spectrum of the chromomycin/d(ATGCAT)$_2$ complex, 15 °C.

for nucleotides alone (Scheek et al., 1983, 1984; Reid et al., 1983; Clore & Gronenborn, 1983), but slightly modified to account for the spectral properties of this system.

A NOESY plot with boxed subregions of the CRA/d-(ATGCAT)$_2$ complex is shown in Figure 5. The first step of the strategy is to identify the CH6–CH5 cross-peaks, which are the most intense cross-peaks in the NOESY spectrum (box a, Figures 5 and 6). This assignment is confirmed by the corresponding cross-peaks in the HOHAHA and COSY plots. Immediately, it is clear that the drug has lifted the dyad symmetry of the duplex. The next step is to identify the thymine 5-CH_3 and H6 resonances by their strong NOESY contacts (box b, Figures 5 and 7). For duplexes alone, the four-bond coupling between these protons can be observed, but we were unable to detect these contacts in any COSY or HOHAHA experiment on the drug complex. Just as for the cytosines, there is one cross-peak for each thymine, indicating the asymmetry induced by the drug affects the whole duplex.

Once these initial assignments are made, all the assignments of the base protons may be made through their contacts to the H1′ resonances (box a, Figures 5 and 6) and the H2′ and H2″ resonances (box b, Figures 5 and 7). Assuming the duplex retains a near-right-handed conformation with deoxynucleosides in the anti conformation, then base proton to 3′-linked sugar H1′, H2′, and H2″ protons and base proton to 5′-linked thymidine methyl and to 5′-linked cytidine H5 protons are all ≥0.50 nm and unobservable as NOE contrasts. Base proton to 5′-linked H1′, H2′, and H2″ are all <0.45 nm and thus observable as NOE contacts (Noggle & Schirmer,

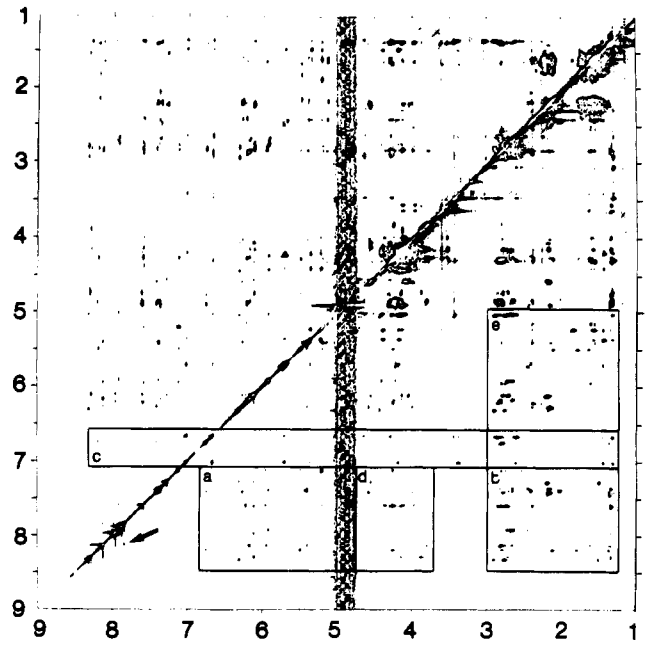

FIGURE 5: ^{1}H NOESY spectrum (mixing time 250 ms) of CRA/d-(ATGCAT)$_2$, 4 mM, in pH 8.2 100 mM phosphate, 180 mM NaCl, 0.2 mM EGTA, and 20 mM Mg^{2+} at 15 °C. Expanded regions described in the text are indicated by boxes and labeled a–e. The arrow indicates the interstrand A_i^aH2–A_t^bH2 cross-peak.

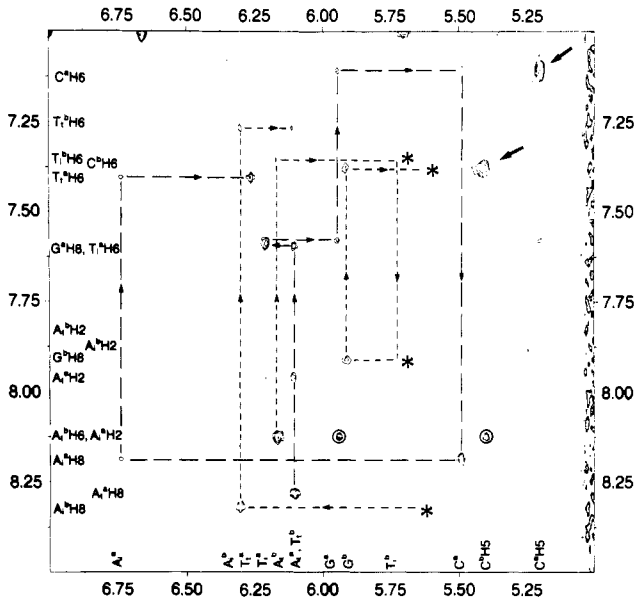

FIGURE 6: Expanded ^{1}H NOESY spectrum (mixing time 250 ms) of CRA/d(ATGCAT)$_2$ (1:1) (base proton to anomeric H1′ region), pH 8.2, 15 °C. Obtained as described in the text. The asterisks indicate points at which the sequential mapping procedure breaks down because of a deviation from the standard right-handed DNA conformation with deoxynucleosides in the anti conformation. The arrows indicate the CH6–CH5 contacts. The lines trace the sequential mapping procedure described in the test. (––) a chain; (- - -) b chain.

1971). When these latter contacts are not observed or are weak, there is a distortion away from the right-handed B conformation. The directionality allows one to step from base proton to base proton in the 5′ to 3′ direction via the H1′ and H2′ and H2″ resonances. These connectivities between adjacent base protons are depicted in Figure 6. The line is unbroken for the "a" chain (––) although the CH6–sugar H1′ NOE's are weak. The "b" chain (···) shows breaks in the line at the T_i^bH6 to G^bH8 link and again at the C^bH6 to A_i^bH8 link (Figure 6, marked by asterisks). The T_i^bH6–T_i^bH1' and G^bH8–T_i^bH1' contacts, however, are observed at longer mixing

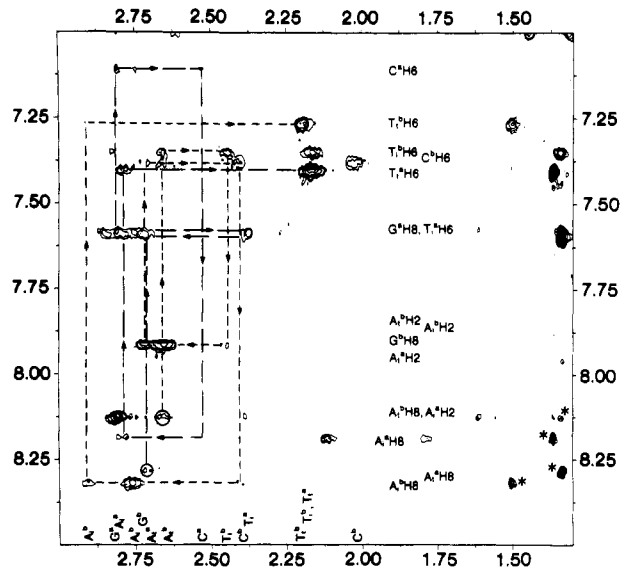

FIGURE 7: Expanded ^{1}H NOESY spectrum (mixing time 250 ms) of CRA/d(ATGCAT)$_2$ (base proton to T-CH_3, anomeric H2′,2″ region), pH 8.2, 15 °C. The asterisks indicate the positions of the AH8 to T5-CH_3 contacts. The lines trace the sequential mapping procedure described in the text. (––) a chain; (- - -) b chain.

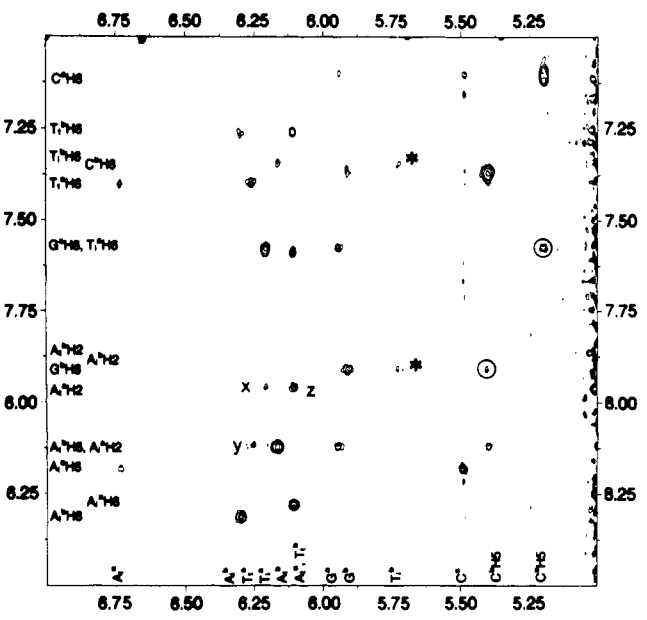

FIGURE 8: Expanded ^{1}H NOESY spectrum (mixing time 400 ms) of CRA/d(ATGCAT)$_2$ (base proton to anomeric H1′ region), pH 8.2, 15 °C. Circled resonances indicate the Cr5 to Cr10 contacts for the a and b chains. The asterisks indicate the T_i^bH6 to T_i^bH1' and G^bH8 to T_i^bH1' contacts, which were missing in the 250-ms NOESY spectrum. The letters x, y, z indicate the T_t^aH1'-A_t^aH2, T_t^aH1'-A_i^aH2, and A_i^aH1'-A_i^aH2 contacts, respectively.

times (400 ms, Figure 8, marked by asterisks). The C^bH^8 to A_i^bH8 connectivity is not observed at 400 ms. These connectivities are also observed, although they are weak, in the 2′ and 2″ region (Figure 7). Clearly, there is a distortion away from the B conformation in the TGCA region of the "b" chain.

One of the four AH2 protons severely overlaps with the A_i^bH8 proton at 8.131 ppm. The other three AH2 protons overlap with the G^bH8 proton but are sufficiently resolved to give distinct cross-peaks in the 2D NOESY spectrum (Figure 5). The AH2 proton at 8.131 ppm is identified as the A_i^aH2 proton by a cross-peak to the H1′ of its 3′-flanking T_t^a thymine residue (y in the 400-ms NOESY spectrum, Figure 8; not observed at a 250-ms mix time, Figure 6); however, a cross-peak is not observed to the H1′ of its own A_i^a sugar. The A_i^aH2

Table II: Chemical Shift (in ppm) Assignments of Nucleotide Base and Sugar Resonances of CRA/d(ATGCAT)$_2$ at 15 °C[a]

	8- or 6-proton	2- or 5-proton	1′	2″,2′	3′
A_t^a	8.287 (8.129)	7.97 (7.825)	6.11 (6.170)	2.72 (2.82, 2.63)	4.80 (4.80)
A_t^b	8.131 (8.129)	7.85 (7.825)	6.17 (6.170)	2.85, 2.69 (2.82, 2.63)	4.87 (4.80)
A_i^a	8.192 (8.310)	8.131 (7.872)	6.75 (6.295)	2.83, 2.74 (2.92, 2.75)	4.89 (5.04)
A_i^b	8.323 (8.310)	7.89 (7.872)	6.31 (6.295)	2.92, 2.78 (2.92, 2.75)	5.03 (5.04)
G^a	7.587 (7.895)		5.95 (5.905)	2.82, 2.75 (2.72, 2.64)	*b* (5.04)
G^b	7.92 (7.95)		5.93 (5.905)	2.75, 2.67 (2.72, 2.64)	5.02 (5.04)
C^a	7.115 (7.371)	5.19 (5.394)	5.49 (5.650)	*b* (2.42, 2.04)	4.82 (4.85)
C^b	7.39 (7.371)	5.44 (5.394)	5.67 (5.650)	2.46 (2.42, 2.04)	*b* (4.85)
T_t^a	7.41 (7.236)	1.37 (1.396)	6.28 (6.111)	2.14 (2.20)	4.59 (4.57)
T_t^b	7.27 (7.236)	1.49 (1.396)	6.116 (6.111)	2.20 (2.20)	4.56 (4.57)
T_i^a	7.598 (7.334)	1.34 (1.263)	6.21 (5.695)	2.38 (2.42, 2.12)	4.88 (4.85)
T_i^b	7.36 (7.334)	1.34 (1.263)	5.73 (5.695)	2.46 (2.42, 2.12)	4.91 (4.85)

[a] Chemical shifts are referenced to internal trimethylsilyl propionate or the water resonance at 15 °C (4.89 ppm). The numbers in parentheses are the chemical shifts of d(ATGCAT)$_2$ in 100 mM phosphate, 180 mM NaCl, and 0.2 mM EGTA, pH 7.0. [b] Could not be assigned.

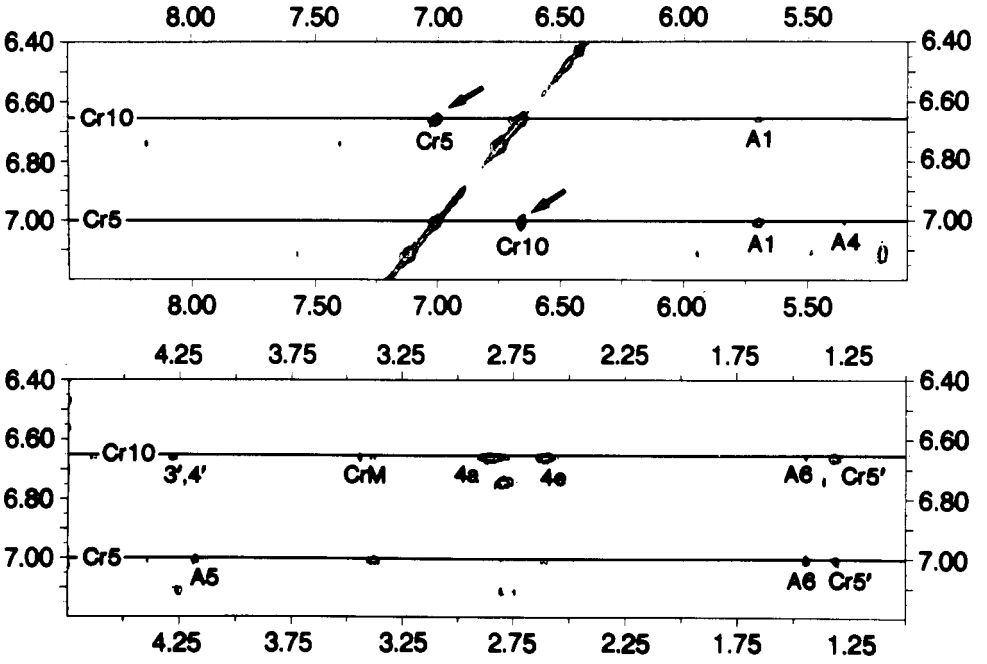

FIGURE 9: Expanded ^{1}H NOESY spectrum (mixing time 250 ms) of CRA/d(ATGCAT)$_2$ displaying the chromomycin H5 and H10 proton NOE contacts, pH 8.2, 15 °C. The arrows indicate the strong Cr5–Cr10 contacts. Cross-peaks with other chromomycin resonances are labeled.

proton also has an interstrand cross-peak to the A_t^bH2 proton at 7.85 ppm (labeled by an arrow in Figure 5). Similarly, the AH2 proton at 7.98 ppm is identified as the A_t^aH2 proton by cross-peaks to the A_t^aH1′ proton and the H1′ of the 3′-flanking T_i^a thymine residue (labeled z and x, respectively, the Figure 8). The A_i^bH2 proton is at 7.89 ppm and has a cross-peak to the A_t^aH2 proton adjacent to the diagonal. Further support for a right handed conformation, albeit distorted, is given by the AH8 to T5-CH_3 cross-peaks (Figure 7, marked by asterisks), which are strong except for the A_t^bH8 to T_i^b5-CH_3 contact. Also of interest is the presence of CH5 to GH8 contacts (circled, Figure 8) on both strands at the 400-ms mixing time. This is clear evidence that the drug does not extensively penetrate between the two G-C pairs since it places an upper limit of 0.45 nm for the G-C base-pair separation. Intercalation of the drug would require a base-pair separation of 0.70 nm. Also evident from Figure 6 is a variability of intensities for cross-peaks of the base 6- or 8-protons to their own H1′ protons, indicating a range of deviation from the anti conformation (we are at present calculating proton–proton distances for this complex from the time-dependent buildup of NOE data. The quantitative results will appear in a future publication).

All the assignable chemical shifts of the nucleotide within the complex are summarized in Table II. The largest chemical shift deviations appear for the T_iGCA_i section of the "a" chain. Particularly large are the chemical shift changes for G^a H8 ($\Delta\delta$ = –0.31), C^aH6 ($\Delta\delta$ = –0.26), C^aH5 ($\Delta\delta$ = –0.20), and T_i^aH6 ($\Delta\delta$ = 0.26). The changes in the corresponding resonances along the "b" chain are small: G^bH8 ($\Delta\delta$ = 0.03), C^bH6 ($\Delta\delta$ = 0.02), C^bH5 ($\Delta\delta$ = 0.05), and T_i^bH6 ($\Delta\delta$ = 0.03). A similar trend is observed for the H1′ residues of the "a" chain, the largest deviations occurring for T_i^aH1′ ($\Delta\delta$ = 0.52), C^aH1′ ($\Delta\delta$ = –0.16), and A_i^aH1′ ($\Delta\delta$ = 0.46). All the chemical shift deviations are summarized in Table III. In contrast, the binding of netropsin to d(GGAATTCC)$_2$ causes large changes in the chemical shifts of the purine H2 protons in the minor groove but only small shift changes in the shifts of the purine H8 protons in the major groove.

Chromomycin Resonances and Drug–Drug Interactions. The spectrum of chromomycin A_3 alone in $CDCl_3$ has been previously assigned (Thiem et al., 1979) and provides an initial basis for the assignment of the drug protons. We use the same numbering scheme as Thiem et al. (Figure 4A); further details are given in the figure legends. The chromomycin chromophore Cr5 and Cr10 protons are easily identified in the downfield region by their mutual high-intensity cross-peaks (Figure 9, marked by arrows), resulting from the short internuclear distance of 0.24 nm. They may be distinguished from each other by cross-peaks to the geminal Cr4 protons

Table III: Chemical Shift Deviations (in ppm) of Nucleotide Base and Sugar Resonances of CRA/d(ATGCAT)$_2$ from the Corresponding Resonances of d(ATGCAT)$_2$

	8- or 6-proton	2- or 5-proton	1′	3′
a chain				
A_t^a	0.16	0.15	−0.06	0.00
T_i^a	0.26	0.08	0.52	0.03
G^a	−0.31		0.05	*a*
C^a	−0.26	−0.20	−0.16	−0.03
A_i^a	−0.12	0.26	0.46	−0.15
T_t^a	0.17	−0.03	0.17	0.02
b chain				
A_t^b	0.00	0.03	0.00	0.07
T_i^b	0.03	0.08	0.04	0.06
G^b	−0.03		0.03	−0.02
C^b	−0.02	0.05	0.02	*a*
A_i^b	0.01	0.02	0.02	−0.01
T_i^b	0.03	0.10	−0.01	−0.01

[a] Could not be assigned for the complex CRA/d(ATGCAT)$_2$.

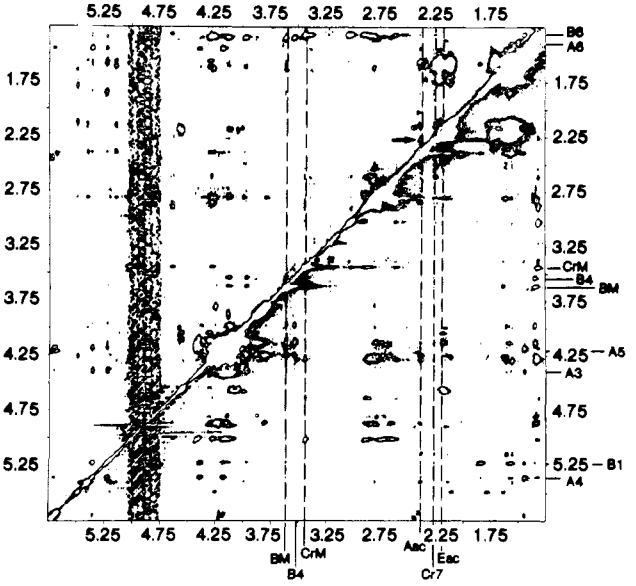

FIGURE 10: Expanded ^{1}H NOESY spectrum (mixing time 250 ms) of CRA/d(ATGCAT)$_2$ showing the contacts to the methoxy, acetyl, and chromophore methyl protons: BM (B sugar methoxy), CrM (chromomycin aliphatic chain methoxy), B4 (B sugar 4-proton), A_{ac} (A sugar acetyl), E_{ac} (E sugar acetyl), and Cr7 (chromomycin chromophore methyl).

on the chromophore at 2.87 and 2.64 ppm [labeled 4a and 4e by Thiem et al. (1979)], which will by strong only for the chromophore Cr10 proton (6.67 ppm). Chromomycin has five methyl groups, which because they are part of functional groups are shifted downfield of the major band of methyl protons at ~1.35 ppm. The two methoxy groups are easily found in the 1D spectrum at 3.62 and 3.448 ppm. Similarly, the two acetyl methyl groups and the chromophore methyl group may be found at 2.39, 2.20, and 2.27 ppm, respectively. The methoxy methyl groups are excellent starting points for a sequential mapping procedure, similar to ones previously used for proteins (Wagner & Wuthrich, 1982) and nucleic acids (Scheek et al., 1983, 1984; Reid et al., 1983; Clore & Gronenborn, 1983). The B sugar methoxy methyl (BM in Figure 10) may be distinguished from the chromomycin aliphatic chain methoxy (CrM in Figure 10) by the cross-peaks to three nuclei at chemical shifts between 3.5 and 4.2 ppm. These are expected to be the B sugar H5, H3, and H4 protons (henceforth referred to as the B5, B3, and B4 protons, respectively). The B4 proton also has cross-peaks to the B3 and B5 protons. The aliphatic chain methoxy methyl (CrM, Figure 10) might be expected to have cross-peaks to the Cr1′, Cr3′, and Cr3

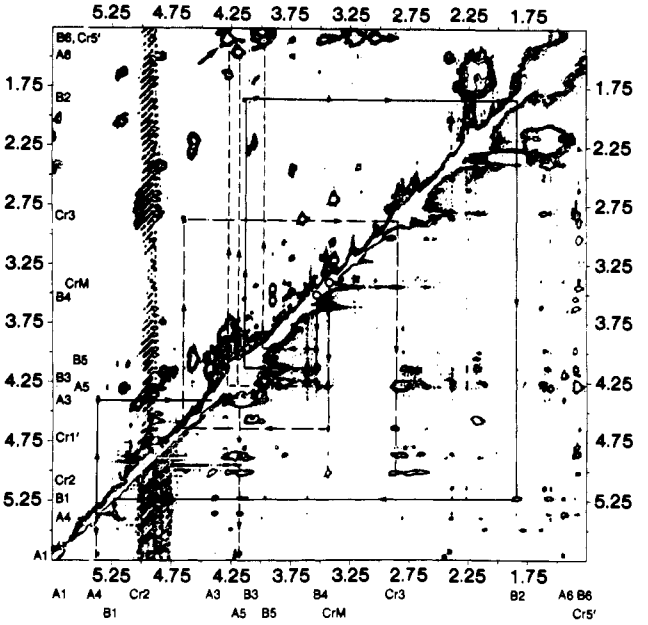

FIGURE 11: A combined NOESY–HOHAHA plot (HOHAHA, upper half; NOESY, lower half) displaying the sequential mapping procedure used to assign the A and B sugar protons: (—) B4 to A1 protons; (---) 4-CH_3 to 5-CH_3 to 6-CH_3 protons and A5 to A1 and A4 to A1 protons; (−−) aliphatic chain protons. The arrow indicates the Cr4′ to Cr5′-CH_3 *J* connectivity.

protons, for which chemical shifts of 4.69, 4.24, and 2.61 ppm, respectively, were reported (Thiem et al., 1979) for this drug dissolved in $CDCl_3$. We find cross-peaks at 4.29 and 4.64 ppm along the CrM line at 3.45 ppm, which we assign to the chromomycin 3′ (Cr3′) and 1′ (Cr1′), respectively. The sequential mapping strategy makes use of a combined NOESY–HOHAHA plot to "walk" from the B4 proton to the A1 proton, in analogy to the procedure used for walking from the NH_{i+1} proton to the NH_i proton in proteins (Wagner & Wuthrich, 1982), by making use of the through-space connectivities of a NOESY plot and through-bond *J* connectivities of a COSY plot. We utilize the HOHAHA plot (Davis & Bax, 1985) because of its superior signal to noise and resolution over a normal COSY plot (Figure 11). The procedure involves walking from the B4 proton to the B3, B2, and B1 protons; then a strong NOE is found between the B1 and A4 protons, and the procedure is repeated again for the A sugar. (The procedure is indicated by the solid line in Figure 11.) There is a break in the procedure at the A3–A2 *J* connectivity (we are unable to observe the *J* connectivity for several 3 to 2′,2″ or 1 to 2′,2″ resonances, in particular to the 1′–2′,2″ of the cytidines). However, the A5 proton is identified by its strong NOE to the A4 proton, and the A1 proton is identified by an NOE to the A5 proton and a weak NOE to the A4 proton. In both the A and B sugars, the 5-proton may be identified by the strong NOE to the 4-proton and the sugar 6-CH_3 protons by the *J* connectivity to the 5-protons (indicated by the dashed lines in Figure 11).

The remaining chromomycin aliphatic chain resonances may be identified by the connectivity and/or through-space interaction with the previously assigned Cr1′ and Cr3′ protons (indicated by the broken line in Figure 11). This connectivity is indicated by the dashed line in Figure 11. Apparently, the 3′-proton is unresolved from the 4′-proton since this resonance also has a *J*-connected cross-peak at 1.33 ppm (arrowed cross-peak in Figure 11), which was confirmed to be a directly coupled cross-peak from the COSY experiment (data not shown). This can only be the Cr4′ to Cr5′-CH_3 cross-peak.

Table IV: ^{1}H Resonance Assignments of Chromomycin A_3 When Complexed to d(ATGCAT)$_2$ at 15 °C

proton	chemical shift (ppm)	proton	chemical shift (ppm)
aglycon		carbohydrate A	
Cr2	5.02 (4.72)[a]	A1	5.70 (5.24)
Cr3	2.86 (2.61)	A2	*c* (2.1)
Cr4a	2.85 (3.07)	A3	4.40 (4.02)
Cr4e	2.60 (2.67)	A4	5.36 (5.16)
Cr5	7.01 (6.55)	A5	4.19 (3.81)
Cr10	6.66 (6.69)	A6-CH_3	1.45 (1.24)
9-OH	16.10 (15.75)	carbohydrate B	
Cr7	2.27 (2.17)	B1	5.23 (5.03)
Cr1′	4.63 (4.69)	B2	1.84 (2.0)
Cr3′	4.29 (4.24)	B3	4.15 (3.89)
Cr4′	4.29 (4.35)	B4	3.55 (3.20)
Cr5′-CH_3	1.32 (1.34)	B5	3.98 (3.87)
functional groups		B6-CH_3	1.34 (1.25)
BM	3.62 (3.56)[b]		
CrM	3.45 (3.50)[b]		
AaC	2.39 (2.16)[b]		
Eac	2.20 (2.12)[b]		

[a] Numbers in parentheses for CRA in CD_2Cl_2 (Thiem et al., 1979). [b] Not assigned to a specific resonance in the original reference. [c] Could not be assigned.

Three methyl groups are observed in the 1D spectrum at 2.39, 2.27, and 2.20 ppm. These peaks belong to the two acetyl methyl groups and the chromomycin chromophore methyl group (denoted A_{ac}, E_{ac}, and Cr7, respectively). The peaks at 2.39 and 2.27 ppm have NOESY cross-peaks to several species on the A and B sugars (including B1 and B3) (Figure 10) and to themselves (arrowed cross-peak in Figure 10), indicating that they are spatially very close. The only conceivable assignment for these two peaks is A_{ac} and Cr7. Of these, only the peak at 2.39 ppm has cross-peaks to the A4 and A5 protons, indicating this must be the A_{ac} proton. The E_{ac} peak at 2.20 ppm has no easily resolvable cross-peaks to other resonances, making the assignment of the C, D, and E sugar protons more difficult.

Although certain patterns are recognizable for the C, D, and E sugar proton resonances, a complete assignment for these resonances is not possible from the available data, and we defer assignment to a future publication. All the resonance assignments of chromomycin are summarized in Table IV.

We may now use the partial assignment of the drug resonances and the NOESY data (Figures 9 and 10) to determine a qualitative picture of the conformation of chromomycin within the complex. The drug aliphatic chain must be partially folded back over the two aromatic protons on the chromophore since NOE's are observed from the 5- and 10-protons to the 3′ and/or 4′ resonance and the 5′-CH_3 resonance of the aliphatic chain. The A sugar has several cross-peaks to the Cr5 resonance; in particular, the A1 proton has a strong cross-peak with the Cr5 proton (Figure 9) but does not have a cross-peak to the Cr7 methyl group. This places the A1 proton proximal to the chromophore aromatic protons but distal to the chromophore methyl group. Furthermore, NOE contacts from the Cr7 to the B1 and B3 protons indicate the B sugar has folded back toward the chromophore 7-methyl group.

Drug–Nucleic Acid Interactions. The most striking aspect of the NOESY plot is the small number of contacts between the drug and the nucleic acid considering the total number of protons in both species. There are no contacts between the drug aromatic protons (Cr5, Cr10) or the aliphatic chian protons (Cr1′, Cr3′, Cr4′, Cr5′) and the nucleic acid base protons, suggesting the aromatic proton side of the chromophore is oriented away from the nucleotide fragment into the external environment. Indeed, the bulky nature of the aliphatic

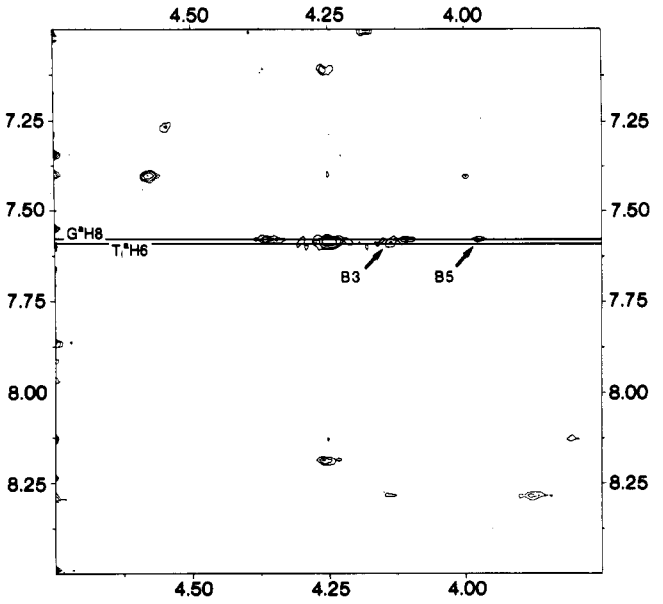

FIGURE 12: Expanded ^{1}H NOESY spectrum of CRA/d(ATGCAT)$_2$ indicating the G^{a}H8 to B sugar contacts. The arrows indicate the contacts between the G^{a}H8 and the B3 and B5 protons.

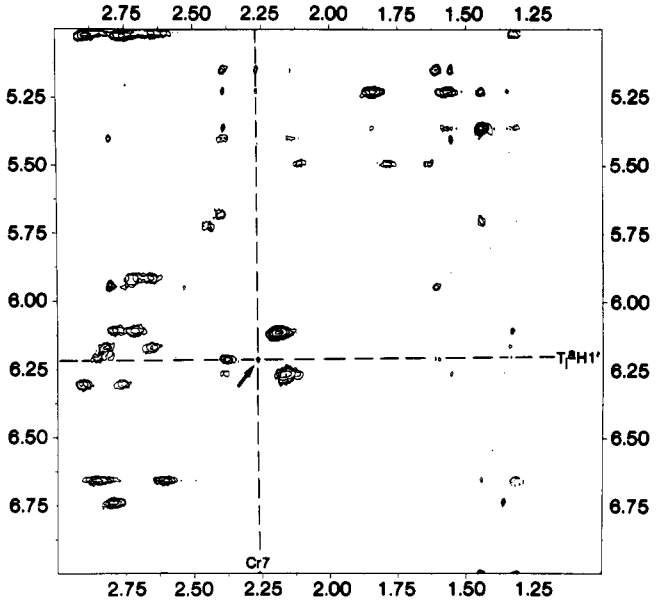

FIGURE 13: Expanded ^{1}H NOESY spectrum of CRA/d(ATGCAT)$_2$. The arrow indicates the T$_i^a$H1′ to Cr7 contact.

chain, which partially overlays the aromatic protons, makes it inconceivable that the drug could intercalate fully between any of the base pairs in the manner of actinomycin (Brown et al., 1984; Jain & Sobell, 1972). There are several cross-peaks between the G^{a}H8 and T$_i^a$H6 resonances and some sugar resonances (Figure 12), some of which no doubt come from 3′ and 4′ nucleotide sugar resonances, but the intensity and number of cross-peaks are too large to come solely from these sources. The two upfield cross-peaks (Figure 12, arrowed) are tentatively identified as the B3 and B5 protons.

The chromomycin chromophore methyl (Cr7) has a cross-peak to only one resolved nucleotide peak, i.e., T$_i^a$H1′ (Figure 13, arrowed cross-peak). In right-handed DNA the nucleotide sugar H1′ points toward the minor groove side of the helix. However, relatively small conformational changes could lead to its contacting the chromophore in the major groove. From model building experiments and the evidence presented here, it seems unlikely that the drug is inserted through the minor groove particularly since there would be

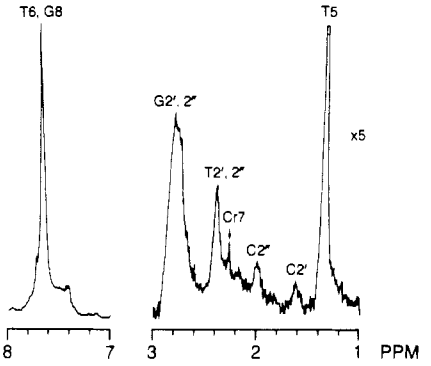

FIGURE 14: NOE difference spectra after 400-ms preirradiation at 7.59 ppm (an envelope that includes the T_i^aH6 and G^aH8 resonances) of CRA/d(ATGCAT)$_2$ in pH 8.2 100 mM borate, 180 mM NaCl, and 20 mM Mg^{2+} at 15 °C. The purine H8 base protons had been partially deuterium exchanged (60%) by incubating the duplex in pH 7.0 100 mM borate, 180 mM NaCl, 4 mM Mg^{2+}, and D_2O buffer at 75 °C for 6 h. The spectrum required 1320 scans at a recycle time of 5.8 s over a 5000-Hz sweep width. An exponential line broadening of 2 Hz was used. The arrow indicates the position of the chromomycin chromophore methyl resonance.

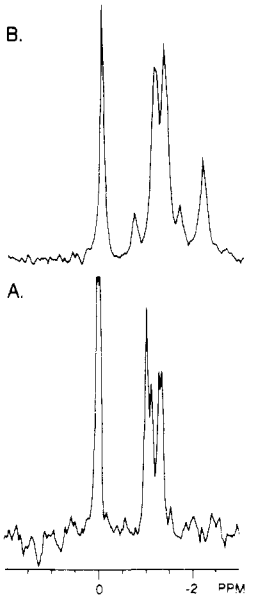

FIGURE 15: ^{31}P spectrum of (A) d(ATGCAT)$_2$ in pH 8.2 borate buffer, 15 °C, and (B) CRA/d(ATGCAT)$_2$ in pH 8.2 borate buffer, 15 °C. Experimental details are in the text.

substantial steric hindrance from the sugar–phosphate backbone. Furthermore, presaturation of the exchangeable chromomycin 9-hydroxy proton did not reveal cross-relaxation to any duplex base protons (data not shown), although we attempted this experiment several times at CRA/d(ATGCAT)$_2$ concentrations up to 6 mM. The other possibility is a conformational change in the nucleotide such that the T_i^aH1' is oriented more toward the major groove, and the Cr7 methyl group is oriented such that it is further than 0.40 nm from the G^aH8 and T_i^aH6. Since these latter resonances overlap and are well separated from any other base protons, a 1D NOE experiment was possible. Presaturation of the resonance at 7.59 ppm produced the cross-relaxation pattern in Figure 14. Although we performed the experiment with the same CRA/d(ATGCAT)$_2$ sample used from the 2D experiment, the cross-relation peak for the chromomycin methyl was best resolved for a sample in which the purine 8-protons had been deuterium exchanged with D_2O prior to the creation of the complex. The level of exchange was estimated to be 60%. The line width of the peak at 2.27 ppm indicates clearly that the resonance arises from an uncoupled methyl group. This places the chromomycin methyl between 0.4 and 0.45 of either the T_i^aH6 or G^aH8 and places the chromophore in the major groove. This chromophore ring position explains the relatively large chemical shift deviations of the "a" chain base protons and especially the large shift deviation for T_i^aH1' ($\Delta\sigma$ = 0.52 ppm) since it places the two aromatic rings of the chromophore proximal to the "a" chain protons and the saturated ring of the chromophore proximal to the "b" chain protons. A major groove location is also in agreement with tentative assignment of the B sugar contacts in Figure 12 and recent footprinting studies (Fox & Howarth, 1985).

The resonances at 8.131 ppm (A_t^bH8 and A_t^aH2) have two cross-peaks (at 5.95 and 5.40 ppm, circled in Figure 6) that are unassigned. The resonance at 5.95 ppm overlaps with the G^aH1' resonance, which could not account for the cross-peak with either A_t^aH2 or A_t^bH8. Similarly, the resonance at 5.40 ppm overlaps with C^bH5 since the latter resonance could not account for a cross-peak with either A_t^aH2 or A_t^bH8. The most likely candidates for these unassigned cross-peaks are the C1, D1, or E1 resonances although at this point we are unable to unequivocally assign these peaks.

In the foregoing discussion we have not considered the role of magnesium ion in the binding of the drug to the nucleotide since we have no direct evidence for the position of the Mg^{2+} ion. However, the unusual location of the chromophore to one side of the helix may be determined by a salt bridge, mediated by Mg^{2+} between the O6 of guanine and the ionizable hydroxyl at position 8 on the chromomycin chromophore (The backbone phosphate group is too distant to form a strong salt bridge with the 8-hydroxyl if the 9-hydroxyl is to be within 0.45 nm of the guanine imino proton; S. Rao, personal communication). The choice of binding location may be determined by the affinity of the 9-hydroxyl of chromomycin for the guanine imino. The most puzzling observation of chromomycin complexes with DNA is the absolute requirement for a 2-aminopurine residue. A major groove location for the drug leaves the 2-amino group with no direct role in the binding of the drug. The role of the 2-amino group may be indirect, simply providing the means to form a third interstrand hydrogen bond, to stabilize the duplex at the binding site from disrupting forces caused by the insertion of the drug.

^{31}P Spectra. ^{31}P NMR of nucleotides may be used to follow changes in the backbone structure and in the case of aromatic drugs the effect of ring currents on nearby phosphate entities. Complex formation of d(ApTpGpCpApT)$_2$ with chromomycin results in the broadening of the two main bands of peaks (at ~−1.0 and ~−1.3 ppm) of the hexanucleotide so that the fine structure is no longer resolved (no doubt due to the longer correlation time of the complex compared to the hexanucleotide alone) and the appearance of three new peaks, one downfield of the main band at −0.696 ppm (integrated area = one phosphorus) and the other two upfield at −1.672 ppm (integrated area = one phosphorus) and −2.154 ppm (integrated area = two phosphoruses) (Figure 15). The ^{31}P spectrum is substantially different from the ^{31}P spectra of the same hexanucleotide complexed to actinomycin (Patel, 1974), a known intercalator, and qualitatively different from the changes in small nucleotide fragments caused by netropsin, a known minor groove binder (Kopka et al., 1985; Patel et al., 1986). Actinomycin, which like chromomycin has mixed aromatic and nonaromatic ring systems, shifts two phosphorus nuclei downfield from the main band. Those nuclei have been assigned to the phosphate resonances at the intercalation site. Netropsin binding results in upfield shifts. Chromomycin does not shift any peak substantially away from the main band, but

it does shift an integrated total of four resonances away from the main band, some upfield and some downfield, implying that this drug binds differently and perhaps has a more disruptive effect on the hexanucleotide structure than actinomycin.

Summary

The data presented above demonstrate that the chromomycin chromophore lies in the major groove of d(ATGCAT)$_2$, in the TG region. The 9-hydroxyl of the drug resides within 0.45 nm of the guanine imino proton, and the orientation of the chromophore ring is such that the hydrophilic side is proximal to the helix center with the chromophore methyl near the TG base protons and the aromatic side is oriented away from the helix. The chromomycin aliphatic chain is oriented such that it partially protects the chromophore aromatic protons from the external solvent. Additional studies are under way with this and other oligonucleotides in order to complete assignments, more fully characterize the ligand–nucleic acid contacts, and elucidate further the nature of the change in DNA conformation at the binding site.

Acknowledgments

We gratefully acknowledge the assistance and advice given by Prof. V. Basus and Dr. R. Scheek, concerning NMR technique and analysis, and a gift of d(ATGCAT) and d(ATICAT) from Dr. Corey Levenson, Cetus Corp., Emeryville, CA.

Registry No. Chromomycin, 74913-06-7.

References

Aue, W. P., Bartholdi, E., & Ernst, R. R. (1976) *J. Chem. Phys. 64*, 2229–2246.

Bakhaera, G., Berlin, Y., Boldyreva, E., Chupronova, O., Kolosov, M., Soifer, V., Vasiljera, T., & Yartsera, I. (1968) *Tetrahedron Lett.*, 3595–3598.

Basus, V. J. (1984) *J. Magn. Reson. 60*, 138–142.

Bax, A., Freeman, R., & Morris, G. (1981) *J. Magn. Reson. 42*, 164–168.

Behr, W., & Hartmann, G. (1965) *Biochem. Z. 343*, 519–527.

Berlin, Y., Espinov, S., Kolosov, M., & Shemyakin, M. (1966) *Tetrahedron Lett.*, 1643–1647.

Braun, W., Bosch, C., Brown, L. R., Gō, N., & Wuthrich, K. (1981) *Biochim. Biophys. Acta 667*, 377–396.

Brown, S. C., Mullis, K., Levenson, C., & Shafer, R. H. (1984) *Biochemistry 23*, 403–408.

Cerami, A., Reich, E., Ward, D., & Goldberg, I. (1967) *Proc. Natl. Acad. Sci. U.S.A. 57*, 1036–1042.

Clore, G. M., & Gronenborn, A. M. (1983) *EMBO J. 2*, 2109–2115.

Cobreros, G., Lopez Zumel, M. C., & Usobiaga, P. (1982) *Radiat. Res. 92*, 255–267.

Davis, D. G., & Bax, A. (1985) *J. Am. Chem. Soc. 107*, 2820–2821.

Feigon, J., Denny, W. A., Leupin, W., & Kearns, D. R. (1984) *J. Med. Chem. 27*, 450–465.

Freeman, R., & Morris, G. A. (1979) *Bull. Magn. Reson. 1*, 5–26.

Fox, K. R., & Howarth, N. R. (1985) *Nucleic Acids Res. 13*, 8695–8714.

Gause, G. F. (1965) *Adv. Chemother. 2*, 179–194.

Hore, P. J. (1983) *J. Magn. Reson. 55*, 283–300.

Horwitz, K. B., & McGuire, W. L. (1978) *J. Biol. Chem. 253*, 6319–6322.

Imai, Y., Ochai, H., Takizawa, H., Shigeno, N., & Koboyashi, Y. (1970) *Niigata Igakkai Zasshi 84*, 715–731.

Jain, S. C., & Sobell, H. M. (1972) *J. Mol. Biol. 68*, 1–20.

Kersten, H., & Kersten, W. (1974) *Mol. Biol. Biochem. Biophys. 18*, 86.

Kersten, W., & Kersten, H. (1965) *Biochem. Z. 341*, 174–183.

Kersten, W., Kersten, H., Steiner, F., & Emmerich, B. (1967) *Hoppe-Seyler's Z. Physiol. Chem. 348*, 1415–1423.

Kopka, M. L., Yoon, C., Goodsell, D., Pjura, P., & Dickerson, R. E. (1985) *Proc. Natl. Acad. Sci. U.S.A. 82*, 1376–1380.

Lvashenko, V. A., & Kolesnikova, L. P. (1965) *Antibiotiki (Moscow) 10*, 808–816.

Maudsley, A. A., & Ernst, R. R. (1977) *Chem. Phys. Lett. 50*, 368–372.

Miyamoto, M., Kawamatsu, Y., Kawashima, K., Shinohara, M., & Nakanishi, K. (1966) *Tetrahedron Lett.*, 545–552.

Muller, L., Kumar, A., & Ernst, R. R. (1975) *J. Chem. Phys. 63*, 5490–5491.

Narang, S. A., Brousseau, R., Hsuing, H. M., & Michniewicz, J. (1980) *Methods Enzymol. 65*, 610–620.

Noggle, J. H., & Schirmer, R. E. (1971) *The Nuclear Overhauser Effect: Chemical Applications*, Academic, New York.

Patel, D. J. (1978) *Proc. Natl. Acad. Sci. U.S.A. 75*, 5483–5487.

Patel, D. J., & Shapiro, L. (1986) *J. Biol. Chem. 261*, 1230–1240.

Pearson, G. A. (1977) *J. Magn. Reson. 27*, 265–272.

Reid, D. G., Salisbury, S. A., Bellard, S., Shekked, Z., & Williams, D. H. (1983) *Biochemistry 22*, 2019–2025.

Remers, W. A. (1979) in *The Chemistry of Antitumor Antibiotics*, Vol. I, p 133, Wiley, New York.

Scheek, R. M., Russo, N., Boelus, R., Kaptein, R., & van Boom, J. H. (1983) *J. Am. Chem. Soc. 105*, 2914–2916.

Scheek, R. M., Boelens, R., Russo, N., van Boom, J. H., & Kaptein, R. (1984) *Biochemistry 23*, 1371–1376.

Slavek, M., & Carter, S. K. (1975) *Adv. Pharmacol. Chemother. 12*, 1–30.

States, D. J., Harberhorn, R. A., & Ruben, D. J. (1982) *J. Magn. Reson. 48*, 286–292.

Van Dyke, M. W., & Dervan, P. B. (1983) *Biochemistry 22*, 2373–2377.

Wagner, G., & Wuthrich, K. (1982) *J. Mol. Biol. 155*, 347–366.

Wakisaka, G., Uchino, H., Nakamura, T., Sotobayashi, H., Shirakawa, S., Adachi, A., & Sakurai, M. (1963) *Nature (London) 198*, 385–386.

Ward, D., Reich, E., & Goldberg, I. (1965) *Science (Washington, D.C.) 149*, 1259–1263.

Waring, M. (1970) *J. Mol. Biol. 54*, 247–279.

Wuthrich, K., Wider, G., Wagner, G., & Braun, W. (1982) *J. Mol. Biol. 155*, 311–319.